Journal of civil engineering and transport **transEngin**

2023, Volume **5** Number **1** **ISSN 2658-1698, e-ISSN 2658-2120**

DOI: 10.24136/tren.2023.004

STEADY-STATE COMPARISON OF TORQUE VECTORING AND VEHICLE TILT INFLUENCE ON NARROW CAR STEERING CHARACTERISTICS

Krzysztof **Weigel-Milleret** [1*]

[1] Cracow University of Technology, Mechanical Department, Faculty of Motor Vehicles, Jana Pawła II 37, 31-864 Kraków, Poland, e-mail: krzysztof.weigel-milleret@pk.edu.pl, https://orcid.org/0000-0001-9128-3736

Reviewed positively: 30.06.2022

Information about quoting an article:
Weigel-Milleret K. (2023). Steady-state comparison of torque vectoring and vehicle tilt influence on narrow car steering characteristics. Journal of civil engineering and transport. 5(1), 47-56, ISSN 2658-1698, e-ISSN 2658-2120, DOI: 10.24136/tren.2023.004

Abstract – Article compares the roll-to-curve and torque vectoring impact on a steering characteristics. The comparison is based on an adopted for tilt mathematical model with two DOFs. The lateral tire forces are a function of the tire sideslip angle and the angle of tilt. The first chapter contains a description of the vehicle for which a series of road tests and simulations was carried out. Next chapter contains an experimental verification of the mathematical model of the vehicle and the simulation tests carried out. The paper describes the mathematical model of the vehicle used to perform the simulation. The next chapter contains the description and results of steady-state simulations examining the effect of differentiation of driving forces on the steering characteristics and the impact of tilt angle on the steering characteristics. The article ends with the chapter containing the conclusions.
Key words – narrow vehicle, steering characteristics, vehicle tilt, torque vectoring, vehicle modeling

JEL Classification – L62, L63, L90, L92, R41

INTRODUCTION

Due to the increase of transport environmental pollution and the rapid population growth in urban areas, constructors are looking for new solutions for individual transport. The automotive industry is facing an increasing number of new challenges such as new emission limits, increased traffic congestion and limited parking spaces in cities. The average vehicle is still (as it was at the early 20s) a four-wheeled vehicle, the size of which increases every year. It is clear that the current vehicle size is highly underutilized. In Europe, the average number of occupants per vehicle ranges from about 1.4 in Denmark to about 2.7 in Romania [3], and in the United States it is about 1.57 [12]. A narrow one or two seated vehicle can solve the problems described above. The narrow cars are a special kind of microcars. Such a vehicle takes up approximately half the lane width and half of the parking space of a conventional vehicle. However, the narrow track of a narrow vehicle can cause its unstable behavior when cornering. Considering geometry of narrow vehicles, these cars are characterized by a high centre of gravity, which makes roll stability an issue. Accidents involving vehicle rollover often have fatal consequences [15].

One way to reduce the vehicle's rollover risk is to tilt the vehicle into a curve like a motorcycle. Moreover, the tilt reduces the difference in normal load between the wheels of the same axle during cornering and increase the maximum lateral acceleration. But the tilting system is difficult to build. It requires a lot of power because the inertia of the tilted part of the body is significant. Currently two mechanical systems are available to perform the vehicle tilting into the curve [2,7]: Direct Tilt Control (DTC) and Steering Tilt Control (STC):

- at the DTC system a dedicated actuator mounted on vehicle's body provides a torque to tilt the vehicle.
- at the STC the actuator modules the steering angle applied by the driver. Body tilting is achieved by the centrifugal force. STC system strategy is similar to a bicycle or motorcycle rider, who use countersteering. The STC requires a Steer-by-Wire system, or at least an active steering assistance where an electric motor can change the steering angle [9].

Both approaches have to solve some tough technical challenges.

Deciphering and even predicting the driver's intentions and desired turn radius is a major challenge.

In the DTC system, both the tilt angle and steering angle have to be synchronized. In the STC system, predicting the tilt angle is even harder. The only input signal is the steering wheel angle. The actuator has to simultaneously control both tilting and vehicle's radius of turn.

Another method, which allows to reduce the risk of the vehicle rolling and does not require special tilting equipment, is to vary the tangential forces of the tires [6]. Thereby, a change in the steering characteristics can be achieved. The changed steerability (for example, a significant increase of understeer) will force the vehicle to behave in a way, that the risk of overturning will be reduced. Such systems are dedicated primarily to vehicles with high mass and inertia (SUV, trucks). Such vehicles cannot be tilted even with powerful actuator systems. The differentiation of the longitudinal forces is achieved by braking forces in the ESC / ESP systems (Electronic Stability Control / Electronic Stability Program). The braking system can generate high tire force, but this dissipates the kinetic energy of the vehicle. Similar effect can be achieved by the differentiation of drive forces [10]. It has been shown in the author's previous articles, that narrow cars are very susceptible to torque vectoring.

No energy dissipation during the force differentiation based roll mitigation system is active is especially important in electric vehicles. Low energy density in traction battery results in a relatively shorter range compared to similar vehicles of a similar class powered by internal combustion engines.

This article compares the roll-to-curve and torque vectoring impact on a steering characteristics. The comparison is based on a mathematical model with two DOFs. Taking into account the tilt of the vehicle required modification of the model equations. The lateral tire forces are a function of the tire sideslip angle and the angle of tilt. The first chapter contains a description of the vehicle for which a series of road tests and simulations was carried out. Next chapter contains an experimental verification of the mathematical model of the vehicle and the simulation tests carried out. Subsequently, the paper describes the mathematical model of the vehicle used to perform the simulation. The next chapter contains the description and results of steady-state simulations examining the effect of differentiation of driving forces on the steering characteristics and the impact of roll on the steering characteristics. The article ends with the chapter containing the conclusions.

1. TESTED VEHICLE

The test object is a narrow car that was designed and developed in Department of Car Design of the Cracow University of Technology. Vehicle body is a welded space frame with a front suspension subframe covered with body panels. Frame design provides high rigidity and torsialonal stiffness of the body. Vehicle is driven by two electric motors built in the rear wheel hubs. The front suspension is a double pushed arm. The small track of the front axle and dependent front wheel suspension causes that the vehicle in the description can be considered as a three wheeled vehicle delta design.

The rear suspension is a semi-independent suspension based on trailing arms. Its basic technical data is presented in Table 1.

2. STEADY-STATE ROAD TEST

To determine the vehicle steering characteristic and to verify the torque vectoring impact on the steering characteristic constant steering wheel angle road tests were conducted. During the test quasi-static acceleration was carried out. The limitation of the vehicle speed was the maximum lateral acceleration or reaching the safety limit (due to the possibility of overturning the vehicle). The increment of the steering wheel angle as a function of lateral acceleration was chosen to analyze the vehicle steering characteristic. The constant steering angle road test is commonly used to compare different vehicles.

Table 1. Tested vehicle basic data

	Parameter	value	unit
m	Weight	278	kg
l_{12}	Wheelbase	1,6	m
l_1	front axle to the center of mass distance	1,03	m
b	track width	0,82	m
h	center of mass height	1,06	m
I_z	z axis moment of inertia	80	kgm^2
K1	front axle sideslip stiffnesses coefficient	9000	N/rad
K2	rear axle sideslip stiffnesses coefficient	18000	N/rad
Kθ	camber stiffnesses coefficient	2500	N/rad

During the test three states of torque distribution were taken into account:

- Equal torque distribution between drive wheels
- Drive force transferred on the outer wheel in relation to curve
- Drive force transferred on the inner wheel in relation to curve.

The following sensors was installed in the vehicle during tests:

- Datron Corrsys Correvit S-CE type L + Q optical sensor measuring the longitudinal and lateral velocities of the vehicle
- Crossbow block measuring lateral and longitudinal velocities, yaw, roll, pitch rates and accelerations
- Honeywell RTY 270HVNAX Rotary sensor measuring steering wheel angle
- Racelogic V-box apparatus. It is a device for measuring the coordinates of a point associated with a vehicle. V-box measurement is based on satellite navigation (GPS and GLONASS) and the inertial component, thanks to which the device calculates the speed, yaw rate and roll speed.
- digital clamp meters measuring the currents supplying electric motors.

Data was transferred by the Spider 8 measuring amplifier. The sampling resolution was 16 bits. The test results were saved on a portable computer. Figure 1 shows tested vehicle equipped with test sensors.

Fig. 1. Tested vehicle during road test (own materials)

3. ROAD TEST RESULT

Performed test shows that the torque vectoring can significantly affects the stability characteristics of the narrow car. En examples of motion paths during the tests are presented in Figure 2. A wide range of differences from understeer to oversteer were obtained. The results on Figure 3 show only the maximum values of the increment of the steering wheel angle as a function of the lateral acceleration.

$$\delta_H - \delta_{H0} = \frac{l_{12}}{R} - \delta_{H0} \tag{1}$$

Where δ_{H0} is steering wheel angle, which is constant during the test.

For the partial distribution of the driving torque, transient characteristics can be obtain. The only limitation is placing them in the marked area on the diagram on Figure 3.

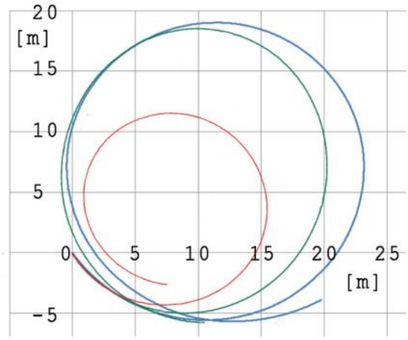

Fig. 2. Motion paths during the tests, (start at 0.0 point); blue - inner wheel drive, green - equal torque distribution, red - outer wheel drive

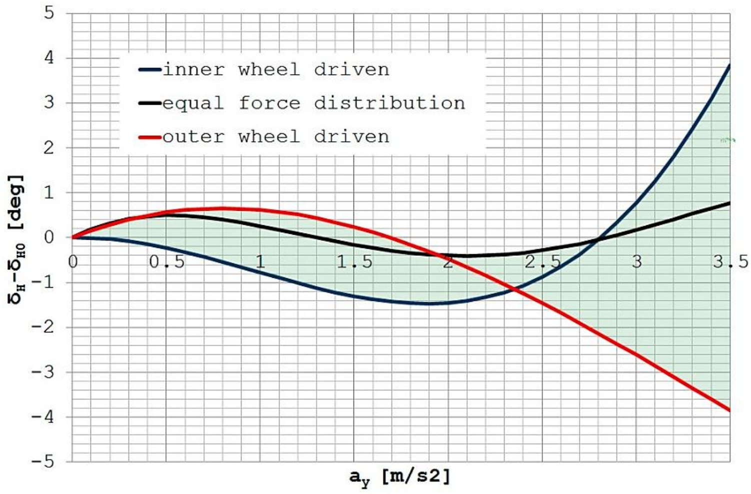

Fig. 3. Driving force distribution influence on steering characteristic

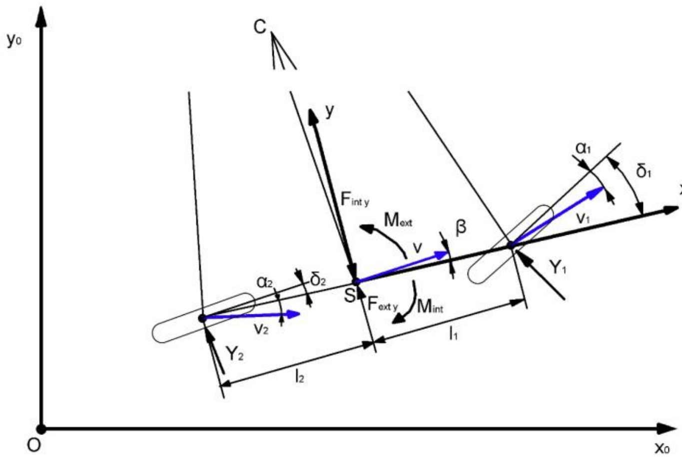

Fig. 4. 2DOF vehicle model

4. VEHICLE MODEL

2 DoFs mathematical model is one of the simplest vehicle model that describes dynamics [8]. The classical 2DoF model assumes that the center of mass of the vehicle is placed on the road surface. Vehicle is regarded as rigid body, the roll and pitch motions are not considered. The rolling and air resistances are neglected. Figure 4 shows the bicycle model geometry on the ground plane.

The vehicle itself is symmetrical about a vertical longitudinal plane and the lateral forces of the tires, the sideslip angles of the left and right tires are assumed to be equal and relatively small, so the axles can be reduced to single wheels. The lateral forces depend only on the sideslip angle. The gyroscopic effect of the wheels is ignored. A serious limitation of that model is ignoring rolling over. For the steady-state conditions the longitudinal velocity is constant (v_x = const), the x-axis motion of the vehicle is not taken into account.

$$\begin{cases} \Sigma F_y = m \cdot \ddot{y} \\ \Sigma M_z = I_z \cdot \ddot{\psi} \end{cases} \tag{2}$$

where F_y and M_z are lateral force and the moment around z axis; y, ψ denote lateral position and yaw angle. The equations of motion take the form:

$$-F_{int\,y} + F_{1y} \cdot \cos\delta_1 + F_{2y} \cdot \cos\delta_2 + F_{ext\,y} = 0 \tag{3}$$

$$-M_{int\,z} + F_{1y} \cdot \cos\delta_1 \cdot l_1 - F_{2y} \cdot \cos\delta_2 \cdot l_2 + M_{ext\,z} = 0 \tag{4}$$

where $F_{int\,y}$ is the inertia force, F_{1y} and F_{2y} are the tires lateral forces, δ_1 and δ_2 are the steering wheel angles on both axles. The lateral inertia force $F_{int\,y}$ and the inertia moment around z axis are:

$$F_{int\,y} = m \cdot \ddot{y} + m \cdot v \cdot \dot{\psi} \cdot \cos\beta + m \cdot \dot{v} \cdot \sin\beta \tag{5}$$

$$M_{int\,z} = I_z \cdot \ddot{\psi} \tag{6}$$

where β is the vehicle sideslip angle. Assuming the linear tire model, the lateral forces for each axle are determined by:

$$\begin{cases} F_{1y} = K_1 \cdot \alpha_1 \\ F_{2y} = K_2 \cdot \alpha_2 \end{cases} \tag{7}$$

where K_1, and K_2 are the sideslip angle stiffnesses for the front and rear axles and α_1, and α_2 are the tire sideslip angles of the front and rear axles. These forces are proportional to the tire sideslip angle. Tire slip angle α is defined as the inverse negative tangent of the tire's lateral to longitudinal velocity ratio. The coefficients of sideslip angle stiffness K are constant values. Such a model is accurate for a small wheel slip $\lambda < 0.15$ and a tire sideslip angle $\alpha < 0.1$ rad [5].

After taking some further assumptions:

$$\begin{gathered} \dot{x} = v = const \\ \delta_2 = 0 \\ \cos\delta_1 = 1 \\ \cos\beta = 1 \\ \beta = \frac{\dot{x}}{\dot{y}} \\ F_{ext\,y} = 0 \end{gathered} \tag{8}$$

inertia force can be presented as:

$$F_{int\,y} = m \cdot \ddot{y} + m \cdot v \cdot \dot{\psi} \tag{9}$$

where $F_{ext\,y}$ is the external lateral force. The differential equations of motion take form:

$$-m\left(v \cdot \dot{\psi} + \ddot{y}\right) + K_1\left(\delta_1 - \frac{\dot{y}}{v} - \frac{l_1 \cdot \dot{\psi}}{v}\right) + K_2\left(-\frac{\dot{y}}{v} - \frac{l_2 \cdot \dot{\psi}}{v}\right) = 0 \tag{10}$$

$$-I_z \cdot \ddot{\psi} + K_1 \cdot l_1\left(\delta_1 - \frac{\dot{y}}{v} - \frac{l_1 \cdot \dot{\psi}}{v}\right) - K_2 \cdot l_2\left(-\frac{\dot{y}}{v} - \frac{l_2 \cdot \dot{\psi}}{v}\right) + M_{ext\,z} = 0 \tag{11}$$

As shown in the literature, torque vectoring can be simulated by an additional yaw moment included in the equation ($M_{ext\,z}$ in Figure 4). The driving force uneven distribution creates additional yaw moment. The simulations presented in the article concern a tilting vehicle in which the lateral forces from the camber are significant. Figure 5 shows the camber angle θ which is defined as the angle between the plane of the wheel and the normal axis to the road surface [11, 1]. In the model used, it was proposed to determine the value of the generated lateral force as a linear function of the wheel tilt. Therefore, the considered lateral force Fy 'can be written as:

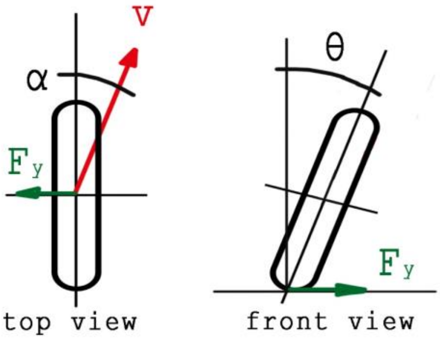

Fig. 5. Slip and camber angles definitions

$$\begin{cases} F_{1y}' = K_1 \cdot \alpha_1 + K_{\theta 1} \cdot \theta \\ F_{2y}' = K_2 \cdot \alpha_2 + K_{\theta 2} \cdot \theta \end{cases} \tag{12}$$

The camber stiffness $K_{\theta n}$, is also a constant value. The equations of proposed model:

$$-m\left(v \cdot \dot{\psi} + \dot{y}\right) + K_1\left(\delta_1 - \frac{\dot{y}}{v} - \frac{l_1 \cdot \dot{\psi}}{v}\right) + K_{\theta 1} \cdot \theta + K_2\left(-\frac{\dot{y}}{v} - \frac{l_2 \cdot \dot{\psi}}{v}\right) + K_{\theta 2} \cdot \theta = 0 \tag{13}$$

$$\begin{gathered} -I_z \cdot \ddot{\psi} + K_1 \cdot l_1\left(\delta_1 - \frac{\dot{y}}{v} - \frac{l_1 \cdot \dot{\psi}}{v}\right) + K_{\theta 1} \cdot \theta \cdot l_1 - K_2 \cdot l_2\left(-\frac{\dot{y}}{v} - \frac{l_2 \cdot \dot{\psi}}{v}\right) \\ -K_{\theta 2} \cdot \theta \cdot l_2 + M_{ext\,z} = 0 \end{gathered} \tag{14}$$

For the special case of steady-state conditions, the accelerations y and ψ are zero and the system of differential equations is simplified to the linear system of equations with two unknowns:

$$\frac{K_1+K_2}{v}\dot{y}+\frac{K_1\cdot l_1-K_2\cdot l_2+m\cdot v^2}{v}\dot{\psi}=K_1\cdot\delta_1+\theta\left(K_{\theta 1}+K_{\theta 2}\right)=0 \tag{15}$$

$$\begin{gathered}\frac{K_1\cdot l_1-K_2\cdot l_2}{v}\dot{y}+\frac{K_1\cdot l_1{}^2-K_2\cdot l_2{}^2}{v}\dot{\psi}=\\=M_{ext\,z}+K_1\cdot l_1\cdot\delta_1+K_{\theta 1}\cdot l_1\cdot\theta-K_{\theta 2}\cdot l_2\cdot\theta=0\end{gathered} \tag{16}$$

Which allows to determine the yaw rate ψ' as a function of the steering angle of the front axle δ, the vehicle tilt angle θ and the additional yaw moment $M_{ext\,z}$. In the tested vehicle, the predetermined values of $K_{\theta 1}$ and $K_{\theta 2}$ were equal and constant, therefore:

$$K_{\theta 1}=K_{\theta 2}=K_\theta \tag{17}$$

$$\dot{\psi}=\frac{v\left(M_{ext\,z}\left(K_1+K_2\right)+K_1\cdot K_2\cdot l_{12}\cdot\delta_1+K_\theta\cdot l_{12}\cdot\theta\left(K_2-K_1\right)\right)}{K_1\cdot K_2\cdot l_{12}{}^2-m\cdot v^2\left(K_1\cdot l_1+K_2\cdot l_2\right)} \tag{18}$$

5. Steering characteristics simulation tests

The simulations of tests with a constant steering angle of the wheels were carried out in accordance with the ISO 4138 standard [13]. It recommends the radius of curvature R=30 m during the test. The simulations were carried out for the steering wheel angle δ_H = 0.214 rad, which corresponds to the front axle steering angle δ_1 = 0.05 rad. The series of simulations included longitudinal speeds in the range v = (0.5;12) m/s, to obtain lateral acceleration a_y > 3.5 m/s^2. The maximum value of lateral acceleration for simulation was selected after calculating the SSF for the test object.

SSF index is commonly used to determine the rollover resistance of a vehicle in a steady-state cornering [14]. This formula allows for the determination of the maximum lateral acceleration value for which none of the vehicle wheels will lose road surface contact. For mass and geometrical parameters of the tested vehicle, the loss of stability lateral acceleration can be obtained. This factor is expressed by the formula:

$$SSF=\frac{b}{2\cdot h} \tag{19}$$

SSF (static stability factor) for tested vehicle is 0.39. The selected value of 3.5 m/s^2 exceeds 90% of the lateral acceleration causing the vehicle to become unstable and separation of the wheels from the road surface.

The above-described mathematical model of the vehicle was used. The geometric and mass parameters of the vehicle were determined at preliminary tests. Previously determined [4] sideslip stiffness and the camber stiffness for the front and rear axles were used in the simulations. The results of the simulation is the yaw rate ψ'. Lateral acceleration a_y, radius of curve R and steering wheel angle increment δ_H - δ_{H0} was calculated.

A series of simulations was carried out for a non-tilting vehicle, without varying the driving forces. This result is nominal to which the others are compared. For such a vehicle, the steering characteristics are almost neutral - the increment of the steering angle $\delta_H - \delta_{H0}$ (a_y = 3.5 m/s^2) = 0.007 rad. The output characteristics of the vehicle are presented in Figure 6.

Simulations were carried out for a tilting vehicle with the same mass and geometrical parameters for the tilt angles θ = 5, 10, 15, 20 deg. Simulation results are presented as functions of longitudinal velocity in Figure 7.

The last series of simulations was performed for a non-tilting vehicle equipped with driving forces differentiation. The amount of the additional deflecting torque (for the purposes of mathematical calculations) was selected on the basis of the vehicle road tests described in point 3. During the tests due to clamp meters, the measurement of currents consumed by the drive motors was done, so the calculation of the driving torque was possible. Driving forces are applied on an arm equal to half the wheel track. It possible to calculate the value of the external moment around z axis, which models the differentiation of driving forces in the single-track model. As the engine drive torques are low, the issues of wheel adhesion and changes in normal loads were ignored. The steering characteristics for these series of simulations are presented as functions of longitudinal velocity in Figure 8. Comparison of all simulations is presented in Figure 9.

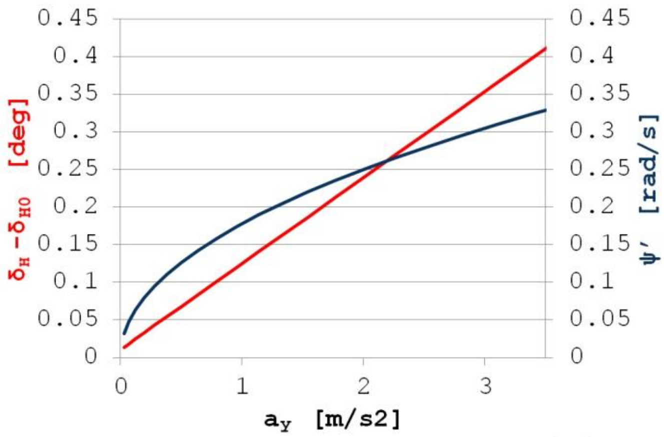

Fig. 6. Steering characteristic of the nontilting vehicle with equal force distribution

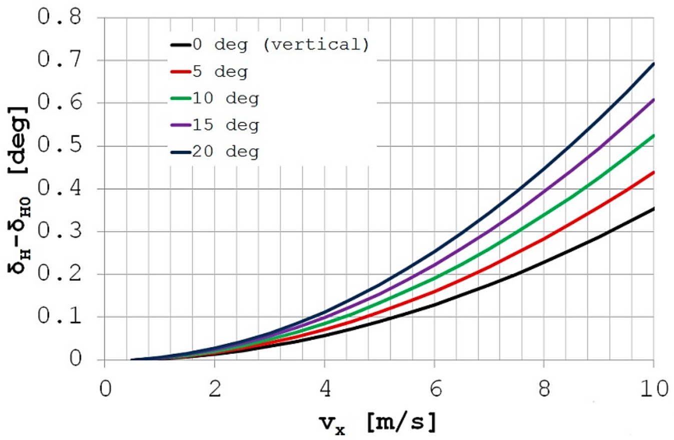

Fig. 7. Steering characteristic of tilting vehicle with equal force distribution

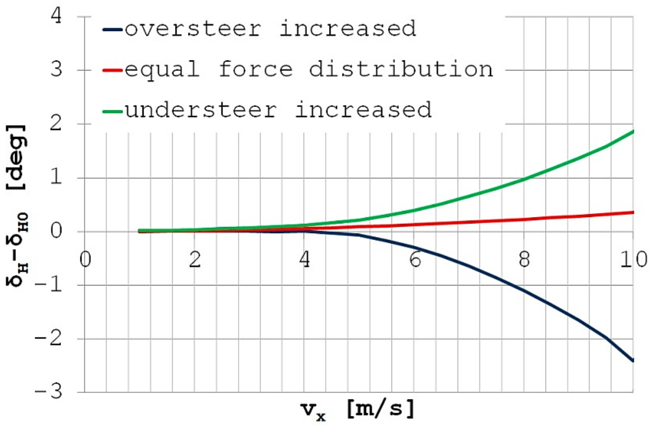

Fig. 8. Steering characteristic of nontilting vehicle with driving forces differentiation

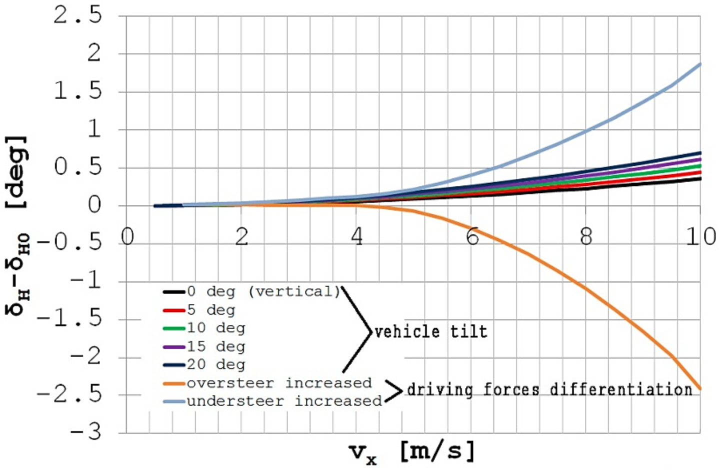

Fig. 9. Steering characteristic comparison

CONCLUSIONS

Road tests of a vehicle equipped with torque vectoring were performed. On their basis, the single-track mathematical model was validated. A proposal to modify the vehicle tire model has been presented. The new model takes into account the tilt of the vehicle and its effect on the forces acting on the vehicle. Tire lateral forces are the sum of the linear function of tire sideslip angle and the linear function of tilt angle. The tests were simulated for a vehicle with the same parameters, taking into account the tilt of the vehicle.

Based on the simulations and road tests, it was found that tilt alone does not significantly affect the vehicle's steerability characteristics. Obviously, tilting the vehicle has the advantage of increasing the rolling resistance. Tilting during cornering reduces the differences in the normal loads on the wheels, and even completely equalizes these loads for the left and right wheels of the vehicle (ideal tilt angle). As is well known, the construction of the vehicle tilting system while driving is complicated, so it is worth looking for alternative systems that improve the stability of narrow vehicle. Steady-state tests show that differentiation of driving forces affects the vehicle's steerability characteristics. Active systems based on differentiation of driving forces allow for any shaping of the steering characteristics. Their main disadvantage is the ability to operate only while delivering driving force to the vehicle, and the limitation for shaping the characteristics is the value of the driving force transmitted to the wheels at a given moment.

PORÓWNANIE WPŁYWU RÓŻNICOWANIA SIŁ NAPĘDOWYCH I PRZECHYŁU POJAZDU NA CHARAKTERYSTYKĘ STEROWNOŚCI WĄSKIEGO POJAZDU W STANIE USTALONYM

Artykuł porównuje wpływ przechyłu i różnicowania sił napędowych na charakterystykę sterowności wąskiego pojazdu. Obiektem badań jest czterokołowy pojazd zbudowany w Katedrze Pojazdów Samochodowych Politechniki Krakowskiej. Wykonano badania drogowe charakterystyk kierowalności pojazdu wyposażonego w różnicowanie sił napędowych. Na ich podstawie dokonano walidacji jednośladowego, zlinearyzowanego modelu pojazdu. Zaproponowano modyfikację liniowego modelu opon pojazdu tak, aby wziąć pod uwagę przechył pojazdu i jego wpływ na siły działajace na pojazd. Siły boczne opony są sumą liniowej funkcji kąta znoszenia opony i liniowej funkcji kąta pochylenia koła. Wykonano symulacje dla pojazdu o takich samych parametrach geometrycznych i masowych dla jazdy po okręgu ze stałym kątem obrotu kierownicy. Badany jest wpływ różnicowania sił napędowych na charakterystykę sterowności oraz wpływ pochylenia pojazdu na charakterystykę sterowności. Na podstawie przeprowadzonych symulacji i testów drogowych stwierdzono, że przechył pojazdu nie wpływa istotnie na sterowność pojazdu w przeciwienstwie do różnicowania sił napędowych. Różnicowanie sił napędowych w wąskich pojazdach potwafi zmienić charakterystykę sterowności od głębokiej podsterwności do nadsterowności. Przechył pojazdu pozytywnie wpływa na odpornośc pojazdu na przewracanie przez zmianę nacisków normalnych pod kołami pojazdu.

Słowa kluczowe: wąski pojazd, charakterystyka sterowności, pojazd przechyłowy, różnicowanie sił napędowych, modelowanie ruchu pojazdu

REFERENCES

[1] Amati N., Festini A., Pelizza L., Tonoli A. (2011). Dynamic modelling and experimental validation of

three wheeled tilting vehicles, *Vehicle System Dynamics*, 49(6,) 889-914, https://doi.org/10.1080/00423114.2010.503277.

[2] Berote J., Darling J., Plummer A. (2012). Development of a tilt control method for a narrow-track three-wheeled vehicle, Proceedings of the Institution of Mechanical Engineers, Part D: *Journal of Automobile Engineering*. 226(1), 48-69. https://doi.org/10.1177/0954407011412311.

[3] Fiorello D., Martino A., Zani L., Christidis P., Navajas-Cawood E. (2016). Mobility Data across the EU 28 Member States: Results from an Extensive CAWI Survey, *Transportation Research Procedia*, 14, 1104-1113, https://doi.org/10.1016/j.trpro.2016.05.181.

[4] Grzegożek W., Zagól B., Kot A. (2019). Analysis of lean angle influence on three wheeled vehicle steerability characteristics, *Research Methods and Solutions to Current Transport Problems*: proceedings of the International Scientific Conference Transport of the 21st Century, 9-12th, June 2019, Ryn, Poland, 1032, 64-172. https://doi.org/10.1007/978-3-030-27687-4_17.

[5] Kaiser G. (2015). Torque Vectoring, Linear Parameter-Varying Control for an Electric Vehicle, PhD Thesis Heidelberg, https://doi.org/10.15480/882.1228.

[6] Kaiser G., Liu Q., Hoffmann C., Korte M., Werner H. (2014). LPV Torque Vectoring for an Electric Vehicle with Experimental Validation, Proceedings of the 19th World Congress *The International Federation of Automatic Control* Cape Town, South Africa. August 24-29, 2014, 12010-12015 https://doi.org/10.3182/20140824-6-ZA-1003.00163.

[7] Karnopp D. (1997). The dynamics of narrow, automatically tilted commuter vehicles. In Proceedings of the EAEC *6th European Congres on Lightweight and small cars – the answer to future needs*, 2–4 July 1997, 13–19. paper no. 97A2KN08.

[8] Kidane S., Alexander L., Rajamani R., Starr P., Donath M. (2008). A fundamental investigation of tilt control systems for narrow commuter vehicles, *Vehicle System Dynamics*, 46(4), 295-322, https://doi.org/110.1080/00423110701352987.

[9] Mourad L., Claveau F., Chevrel P. (2014). Direct and Steering Tilt Robust Control of Narrow Vehicles. *IEEE Transactions on Intelligent Transportation Systems*, IEEE, 2014, 15(3), 1206-1215, https://doi.org/110.1109/TITS.2013.2295684.

[10] Rill G. (2017). Reducing the cornering resistance by torque vectoring, X International Conference on Structural Dynamics, EURODYN 2017 *Procedia Engineering*, 199, 3284 – 3289. https://doi.org/10.1016/j.proeng.2017.09.393.

[11] Yi W., Shuilong H., Enyong X., Genge Z., Rongjiang T., Wei W., Chao L. (2020). Steady-State Steering Characteristics of Mathematical Model for Semitrailer Based on Variations in Camber Parameters, *Shock and Vibration*. 2020, https://doi.org/10.1155/2020/6272397.

[12] FHWA 2017, NHTS Report, *Changing attitudes and transportation choices*, February 2019, Report, U.S. Department of Transportation, https://nhts.ornl.gov/assets/FHWA_NHTS_Report_3E_Final_021119.pdf (access date: 20/05/2021).

[13] ISO 4138:2012 Passenger cars - Steady-state circular driving behaviour - Open-loop test methods.

[14] Trends in the Static Stability Factor of Passenger Cars, Light Trucks, and Vans, NHTSA Technical Report, DOT HS 809 868, 2005.

[15] https://one.nhtsa.gov/ (access date: 02/02/2022).